Supporting Information

Confronting the Invisible: Assignment of Protein $^{1}H^{N}$ Chemical Shifts in Cases of Extreme Broadening

Leo E. Wong,[1,#] Tae Hun Kim[2], Enrico Rennella[1], Pramodh Vallurupalli,[3,#] and Lewis E. Kay[*1,2]

ABSTRACT NMR studies of intrinsically disordered proteins (IDPs) at neutral pH values are hampered by the rapid exchange of backbone amide protons with solvent. Although exchange rates can be modulated by changes in pH, interactions between IDPs that lead to phase separation sometimes only occur at neutral pH values or higher where backbone amide-based experiments fail. Here we describe a simple NMR experiment for measuring amide proton chemical shifts in cases where $^{1}H^{N}$-spectra cannot be obtained. The approach uses a weak ^{1}H B_1 field, searching for elusive $^{1}H^{N}$ resonance frequencies that become encoded in the intensities of cross-peaks in 3D $^{1}H^{\alpha}$-detect spectra. Applications to the CAPRIN1 protein in both dilute- and phase-separated states highlight the utility of the method, establishing that accurate $^{1}H^{N}$ chemical shifts can be obtained even in cases where solvent hydrogen exchange rates are on the order of 1500 s^{-1}.

[1] Departments of Molecular Genetics, Biochemistry and Chemistry, University of Toronto, Toronto, Ontario M5S 1A8, Canada

[2] Program in Molecular Medicine, Hospital for Sick Children, 555 University Avenue, Toronto, Ontario M5G 1X8, Canada

[3] TIFR Centre for Interdisciplinary Sciences, Tata Institute of Fundamental Research Hyderabad, 36/P, Gopanpally Village, Serilingampally Mandal Ranga Reddy District, Hyderabad, Telangana 500107, India

[#] These authors contributed equally to this work.

[*] kay@pound.med.utoronto.ca

Table of Contents

Materials and Methods

Sample preparation

The C-terminal region of CAPRIN1 comprising amino acids 607-709, referred to in this paper as CAPRIN1, was overexpressed and purified as described previously[1,2]. A pair of dilute-phase CAPRIN1 samples (*i.e.*, non phase-separated samples) was prepared for analysis. These included a 0.5 mM protein sample dissolved in 25 mM MES, pH 5.5, 10% D_2O that was used to establish the accuracy of the indirect (SE_haCONHA) approach for measurement of $^1H^N$ chemical shifts, as high quality amide spectra could be directly measured in this case. A second CAPRIN1 sample was produced (0.7 mM protein, 25 mM HEPES, pH 7.4, 2% D_2O) where only poor quality $^1H^N$-^{15}N data sets could be recorded due to rapid solvent hydrogen exchange rates (Figure S1 and S2). Both samples were ^{15}N,^{13}C-labeled and generated by bacterial growth and expression using minimal media comprising 6 g of Na_2HPO_4, 3 g of KH_2PO_4, 0.5 g of NaCl, 1 g of $^{15}NH_4Cl$, 3 g of [U^{13}C]-glucose, 2 mM $MgSO_4$, 50 μg/mL of kanamycin, 10 mg each of biotin and thiamine in 1 L of expression media at pH 7.4. In addition, a condensed-phase (*i.e.*, phase-separated) sample was prepared as described previously[2], with approximately 15 mM protein dissolved in 25 mM NaPi, 100 mM NaCl, pH 7.4, 10% D_2O. A molar ratio of ^{15}N,^{13}C-labeled to unlabeled protein of approximately 1:7 was used for this sample.

NMR spectroscopy

All NMR experiments were recorded on an AVANCE III HD 600 MHz Bruker spectrometer equipped with a 5-mm TCI cryo-probe with x, y, z pulsed field gradients. In addition to SE-haCONHA data sets (Fig. S3), $^1H^N$-detect cross polarization (CP) enhanced HSQC (CP-HISQC[3]) and HNCO experiments were also recorded. The CP schemes exploit rapid solvent hydrogen exchange as a source of ^1H magnetization for the initial polarization transfer (10.8 ms, 4 kHz simultaneous ^1H and ^{15}N fields) from $^1H^N$ to ^{15}N, as described previously[3]. The SE_haCONHA scheme is based on a recently published haCONHA experiment[2] in which polarization both originates from and is detected on the $^1H^\alpha$ proton. It includes an ^{15}N spin-echo element, as illustrated in Figure S3, with the application of a weak ^1H rf field (typically 200-500 Hz) at frequency offsets ranging from ~6-10 ppm (one offset for each data set) during the echo. A series of 3D (^{13}CO, ^{15}N, $^1H^\alpha$) planes (typically 15-20) was recorded, with the $^1H^N$ chemical shift encoded in the intensities of the correlations. Data sets were acquired with non-uniform sampling[4–6] (NUS) of the indirect-detect ^{13}CO and ^{15}N dimensions using Poisson-gap sampling schemes[7].

Each pseudo-4D data set so obtained was processed in one of two ways: (1) As individual 3D data sets reconstructed using the program *SMILE*[8] and analyzed with the *nlinLS* peak-fitting routine in the

NMRPipe software package[9]. All time dimensions were windowed by cosine-bell functions ending at sin(0.98π), with the exception of the directly acquired ^{1}H dimension for the condensed phase sample, where the cosine-bell squared function terminated at 0 and where linear prediction was applied to the ^{15}N-dimension. (2) The pseudo-4D data set was analyzed in the time-domain as described previously[10] and below. The peak list required for the time-domain fitting was obtained by analyzing the reference spectrum (from which initial intensities I_0 are obtained, along with initial estimates of peak positions). We have found that for weak or poorly resolved correlations the peak intensities obtained from analysis of data in the time-domain are more reliable than those from analysis of frequency-domain data.

Time-domain fitting of pseudo-4D data

We have recorded a series of 3D SE_haCONHA data sets, each acquired with a weak ^{1}H cw field (of strength ν_1) applied at a frequency corresponding to between ~6-10 ppm in the ^{1}H dimension. Because approximately 20 3Ds are measured, corresponding to 20 points in the I/I_0 profiles, NUS has been used. Prior to considering the situation with NUS, we first describe the case where the data is uniformly sampled in all dimensions. After Fourier transformation of the detected ^{1}H dimension (^{1}H$^\alpha$) (using *NMRPipe*[9]) a set of 3D matrices is subsequently generated, each at a given ^{1}H$^\alpha$ (ϖ^{H}) frequency of interest (*i.e.*, where there are peaks). Each of these 3D matrices can be written as the tensor product of 3 vectors, two of which are normalized time-evolution vectors $\boldsymbol{v}_j^q$ with $q \in$ [CO,N], and the third vector, $\boldsymbol{w}_j^{\mathrm{H}}$, tabulates the amplitudes of cross peaks for each of the L different positions of the weak ^{1}H B_1 field,

$$\boldsymbol{S}(\boldsymbol{\varpi}^{\mathrm{H}}) = \sum_{j=1}^{J} \boldsymbol{v}_j^{\mathrm{N}} \otimes \boldsymbol{v}_j^{\mathrm{C}} \otimes \boldsymbol{w}_j^{\mathrm{H}} \ , \qquad [\mathrm{S1}]$$

where the summation is over all J cross-peaks that have a ^{1}H resonance frequency within ±0.03 ppm of ϖ^{H}. Eq. [S1] applies not only in the case of uniformly sampled data, but also for NUS sampling, when the NUS schedule is as illustrated in the left panel of the depiction here where the 2D-{^{13}CO, ^{15}N} NUS matrix, of dimensions A x B, comprises all possible combinations from a ^{13}CO NUS sampling vector of length A and an ^{15}N sampling vector of length B. Time-domain fitting for this implementation, in the context of the analysis of CEST data, has been discussed previously[10].

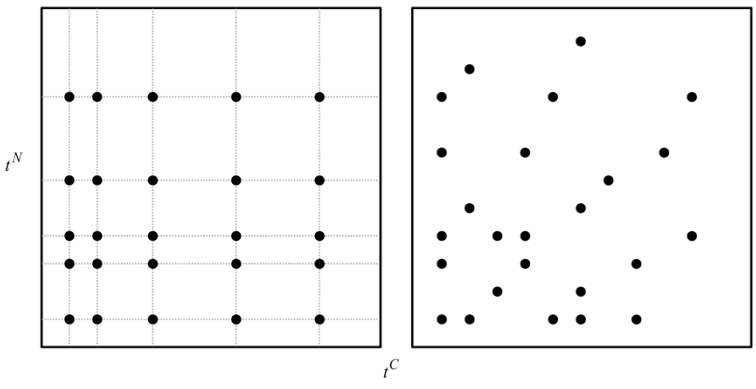

Here we use a sampling matrix that is more general, depicted in the panel on the right of the figure. It can be seen that in this case the NUS schedule is not a simple *A* x *B* matrix given by the tensor product of 1D ^{13}CO and ^{15}N sampling vectors. Rather, time domain signals corresponding to a given ϖ^{H} frequency are described by

$$\boldsymbol{S}(\boldsymbol{\varpi}^{\mathrm{H}}) = \sum_{j=1}^{J} \boldsymbol{v}_j^{\mathrm{CN}} \otimes \boldsymbol{w}_j^{\mathrm{H}} \quad , \qquad \text{[S2]}$$

where the time-evolution of the ^{13}CO and ^{15}N spins are combined into a single column vector, $\boldsymbol{v}_i^{\mathrm{CN}}$, of size $4{\cdot}K$ that includes the 4 quadrature components and the K increments in the NUS sample schedule ($K = 25$ in the example above)

$$\begin{matrix}
v_j^{CO,re}(t_1^{CO}) \cdot v_j^{N,re}(t_1^N) \\
v_j^{CO,im}(t_1^{CO}) \cdot v_j^{N,re}(t_1^N) \\
v_j^{CO,re}(t_1^{CO}) \cdot v_j^{N,im}(t_1^N) \\
v_j^{CO,im}(t_1^{CO}) \cdot v_j^{N,im}(t_1^N) \\
v_j^{CO,re}(t_2^{CO}) \cdot v_j^{N,re}(t_2^N) \\
v_j^{CO,im}(t_2^{CO}) \cdot v_j^{N,re}(t_2^N) \\
v_j^{CO,re}(t_2^{CO}) \cdot v_j^{N,im}(t_2^N) \\
v_j^{CO,im}(t_2^{CO}) \cdot v_j^{N,im}(t_2^N) \\
\vdots \\
v_j^{CO,re}(t_K^{CO}) \cdot v_j^{N,re}(t_K^N) \\
v_j^{CO,im}(t_K^{CO}) \cdot v_j^{N,re}(t_K^N) \\
v_j^{CO,re}(t_K^{CO}) \cdot v_j^{N,im}(t_K^N) \\
v_j^{CO,im}(t_K^{CO}) \cdot v_j^{N,im}(t_K^N)
\end{matrix} \qquad \text{[S3]}$$

$\boldsymbol{w}_j^{\mathrm{H}}$ is a row vector of length L, and $\boldsymbol{S}$ is a 2D matrix of dimensions $4{\cdot}K$ x L. Note that, in contrast to Eq. [S1], $\boldsymbol{S}$ in Eq. [S2] is written as a 2D matrix. In Eq. [S3], the *re* and *im* superscripts indicate real and imaginary components

$$\begin{aligned}
v_j^{q,re}(t_k^q) &= \exp(-R_j^q \cdot t_k^q) \cdot \cos(\boldsymbol{\varpi}_j^q \cdot t_k^q + \varphi^q) \\
v_j^{q,im}(t_k^q) &= \exp(-R_j^q \cdot t_k^q) \cdot \sin(\boldsymbol{\varpi}_j^q \cdot t_k^q + \varphi^q)
\end{aligned} \quad , \qquad \text{[S4]}$$

where $\boldsymbol{\varpi}_j^q$ and R_j^q are the resonance frequency and the transverse relaxation rate for the q spin, $q \in$ [CO, N], of the j cross-peak, respectively, φ^q is the zero-order phase correction in the q dimension, and the subscript k is the index in the NUS sampling schedule ($1 \le k \le K$). To expedite the computation of $\boldsymbol{S}$ it is convenient to rewrite it as

$$\boldsymbol{S}(\boldsymbol{\varpi}^{\mathrm{H}}) = \boldsymbol{V}^{CN} \cdot \boldsymbol{W}^{H}, \qquad \text{[S5]}$$

where $\boldsymbol{V}^{CN}$ is a $(4 \cdot K)$ x J matrix whose elements are derived from Eqs [S3-S4] for all $(4 \cdot K)$ NUS increments such that each column of $\boldsymbol{V}^{CN}$ is given by the elements in Eq. [S3] and there is a separate column for each of the J cross-peaks that have a ^{1}H resonance frequency within ±0.03 ppm of ϖ^{H}. In Eq. [S5] $\boldsymbol{W}^{H}$ is a J x L matrix whose elements are the intensities for all of the J cross-peaks at each of the L ^{1}H irradiation offsets, with each row listing the intensities for a given peak as a function of L. Thus, an I/I_0 profile for residue p ($1 \le p \le J$) is constructed from a set of L $\boldsymbol{W}^{H}$ values, corresponding to the elements of row p of $\boldsymbol{W}^{H}$. In order to illustrate how the simulated $\boldsymbol{S}(\boldsymbol{\varpi}^{H})$ matrices, Eq. [S5], are constructed (that are subsequently compared with experimental data during the fitting stage, see below) suppose that there are 6 peaks of interest at the following ϖ^{H} frequencies,

N	ϖ^{H} *(ppm)*
P1	*4.50*
P2	*4.45*
P3	*4.44*
P4	*4.416*
P5	*4.391*
P6	*4.373*

and that the transformed ^{1}H$^{\alpha}$ dimension has a digital resolution of 0.01 ppm, with peaks within +/- 0.03 ppm of the selected frequency included in the fit. Then 6 $\boldsymbol{S}(\boldsymbol{\varpi}^{H})$ matrices are constructed, to be fit to the experimental data, corresponding to:

ϖ^H (ppm)	Peaks Fit in $\boldsymbol{Sj}$	Peak for which the I/I_0 profile is saved
S1 4.50	P1	P1
S2 4.45	P2,P3	P2
S3 4.44	P2,P3,P4	P3
S4 4.42	P3,P4,P5	P4
S5 4.39	P4,P5,P6	P5
S6 4.37	P5,P6	P6

Note that once the peaks that are included in each $\boldsymbol{Sj}$ are established, $\boldsymbol{V}^{CN}$ can be calculated and $\boldsymbol{S(\varpi^H)}$ determined from Eq. [S5] using initial guesses for the elements of $\boldsymbol{W}^H$. Experimental $\boldsymbol{S(\varpi^H)}$ matrices, to be compared with the simulated $\boldsymbol{S(\varpi^H)}$ matrices, constructed as described above, can be readily generated by converting the initial pseudo-4D data set into a 3D matrix comprising $4{\cdot}K$ indirect detection points (^{15}N,^{13}C; NUS), L frequency positions of the weak B_1 field, and N direct-detection acquisition points (^{1}H$^\alpha$). After Fourier transformation of the acquisition dimension a series of 2D $\boldsymbol{S(\varpi^H)}$ data sets ($4{\cdot}K$ x L) are generated at the ^{1}H$^\alpha$ frequencies of interest. Fitted parameters, that include all the elements of the $\boldsymbol{W}^H$ matrix, as well as ϖ_j^q and R_j^q, are obtained from the minimization of the square of the residuals between experimental and simulated $\boldsymbol{S(\varpi^H)}$ components. Fits are done in two steps. First, the elements of the matrix $\boldsymbol{W}^H$ are allowed to change while ϖ_j^q and R_j^q are constrained to initial values from the analysis of a reference haCONHA data set. Subsequently, ϖ_j^q and R_j^q are allowed to vary, with fine adjustments of the chemical shifts (within ±0.04 ppm for ^{13}CO and ±0.1 ppm for ^{15}N of the starting values). The code for data fitting is available upon request.

Analysis of SE_haCONHA data

During the spin-echo element of duration $2\tau_5$ in Figure S3 (B.2), the evolution of backbone amide ^{15}N magnetization from the combined effects of (i) the one-bond ^{1}H^N-^{15}N scalar coupling ($^1J_{HN}$ = -94 Hz[11]), (ii) solvent hydrogen exchange (rate k_{ex}), and the application of a weak ^{1}H cw field of magnitude ν_1, can be described by the following equations of the density matrix[12–14],

$$\frac{d\boldsymbol{\rho}}{dt} = -\hat{L}\boldsymbol{\rho} \qquad \text{[S6]}$$

so that,

$$\boldsymbol{\rho}(2\boldsymbol{\tau}_5) = e^{-\hat{L}\boldsymbol{\tau}_5} R_{N,H} e^{-\hat{L}\boldsymbol{\tau}_5} \boldsymbol{\rho}(0), \text{ where} \qquad [S7]$$

$$\hat{L} = \begin{pmatrix} 0 & \boldsymbol{\pi}\,{}^1J_{HN} & 0 & 0 \\ -\boldsymbol{\pi}\,{}^1J_{HN} & k_{ex} & 2\boldsymbol{\pi}\nu_1 & 0 \\ 0 & -2\boldsymbol{\pi}\nu_1 & k_{ex} & 2\boldsymbol{\pi}\Delta \\ 0 & 0 & -2\boldsymbol{\pi}\Delta & k_{ex} \end{pmatrix}, \qquad [S8]$$

$$\hat{R}_{N,H} = \begin{pmatrix} -1 & 0 & 0 & 0 \\ 0 & -1 & 0 & 0 \\ 0 & 0 & 1 & 0 \\ 0 & 0 & 0 & -1 \end{pmatrix} \qquad [S9]$$

and ρ is a column vector given by $\{N_y, 2N_xH_z, 2N_xH_y, 2N_xH_x\}^+$, where '+' is the transpose operator. The matrix $\hat{R}_{N,H}$ takes into account the combined effects of the ^{15}N and ^{1}H 180^o pulses, of phases *x* and *y*, respectively, that are applied at the center of the echo, and Δ is the separation (Hz) between the position of the weak ^{1}H B_1 field (ν_1) and the $^1H^N$ resonance frequency of interest. Simulated I/I_0 profiles are calculated numerically from the equations above. Experimental I/I_0 profiles were fit to Eqs. [S7-S9] to extract Δ and k_{ex} (assuming $^1J_{HN}$ = -94 Hz) using an in-house written MATLAB routine that is available upon request. Errors in the experimental points were established on the basis of repeat measurements and subsequently used to estimate uncertainties in the fitted parameters, Δ and k_{ex}, from a Monte Carlo analysis[15] involving 200 simulated data sets.

It is important to note that in the analysis described above we have assumed that the solvent is 100% H_2O. In the applications considered, however, a small amount of D_2O has been added for lock, varying from 2% (dilute samples) to 10% (phase-separated sample). We have carried out a set of simulations to evaluate the errors in extracted k_{ex} values that derive from neglecting contributions involving exchange with D_2O in H_2O/D_2O solvent systems using a set of equations derived by Kateb *et al.*[12]. For 2% D_2O the errors in k_{ex} generated by neglecting the D_2O content in the buffer are very small, on the order of 1-2% for values up to 2000 s^{-1}. The errors are below 10% for a buffer consisting of 10% D_2O/90% H_2O when the solvent composition is neglected. In all cases k_{ex} values are overestimated.

Derivation of Eq. [1]

In the limit that $\nu_1 = 0$ it follows from Eq. [S6] that

$$\frac{dN_y}{dt} = -\pi J_{HN} 2N_x I_z$$
$$\frac{d2N_x I_z}{dt} = \pi J_{HN} N_y - k_{ex} 2N_x I_z \qquad \text{[S10]}$$

This system of equations, Eq. [S10], can be readily solved to give

$$N_y(t) = Ae^{\lambda_1 t} + Be^{\lambda_2 t} \qquad \text{[S11]}$$

$$\lambda_{1,2} = \frac{-k_{ex} \pm \sqrt{k_{ex}{}^2 - (2\pi J_{HN})^2}}{2} = \frac{-k_{ex} \pm 2\pi |J_{HN}| i\sqrt{1-\alpha^2}}{2} \qquad \text{[S12]}$$

where $\alpha = \frac{k_{ex}}{2\pi |J_{HN}|}$ and $i = \sqrt{-1}$.

Imposing the boundary conditions, $N_y(0) = N_{y,o}$, $2N_x I_z(0) = 0$, and using Eq. [S11] we obtain

$$N_{y,o} = A + B$$
$$\left.\frac{dN_y}{dt}\right|_{t=0} = 0 = A\lambda_1 + B\lambda_2 \qquad \text{[S13]}$$

from which it follows that $A = -N_{y,o}\frac{\lambda_2}{\lambda_1 - \lambda_2}$ and $B = N_{y,o}\frac{\lambda_1}{\lambda_1 - \lambda_2}$.

Substituting expressions for *A*, *B* and $\lambda_{1,2}$ into Eq. [S11] we arrive at Eq. [1] of the main text, with $J_{eff} = J_{HN}\sqrt{1-\alpha^2}$.

In the limit where $\alpha \gg 1$ (fast exchange) it is convenient to rewrite $J_{eff} = iJ_{HN}\sqrt{\alpha^2 - 1} = iJ_{HN}|\alpha|\sqrt{1-\frac{1}{\alpha^2}} \approx iJ_{HN}|\alpha|(1-\frac{1}{2\alpha^2})$. Substituting this expression for J_{eff} into Eq. [1] of the main text and simplifying gives

$$N_y(t) = N_{y,o} e^{-\frac{k_{ex}}{4\alpha^2}t} \quad . \qquad \text{[S14]}$$

Supplementary Figures

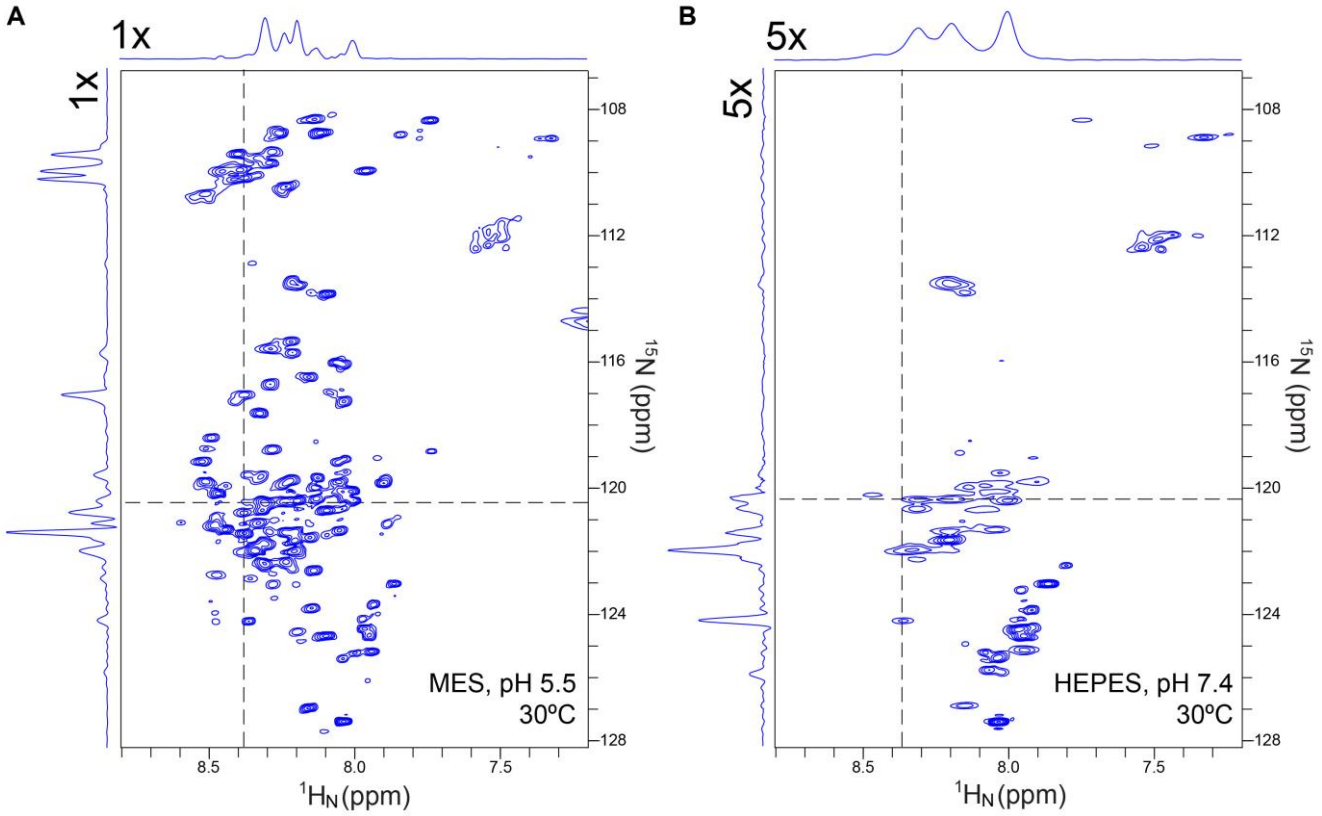

Figure S1. CP-HISQC[3] spectra of dilute phase CAPRIN1 recorded at pH 5.5 and 7.4, 30ºC. 2D cross polarization-enhanced HSQC experiments, optimized for applications to IDPs[3], were measured using identical experimental settings on a pair of CAPRIN1 samples: (A) 25 mM MES buffer, pH 5.5 (0.5 mM) and (B) 25 mM HEPES buffer, pH 7.4 (0.7 mM). The experimental settings were: Interscan relaxation delay = 2 s, $t_{acq,max}$ = 64 ms, $t_{1,max}$ = 55 ms. Traces shown on top and to the left of the spectra (contoured at the same level) were extracted along the dashed lines; note the five-fold multiplication of traces in B. The poor quality of the data set recorded using sample B is clear.

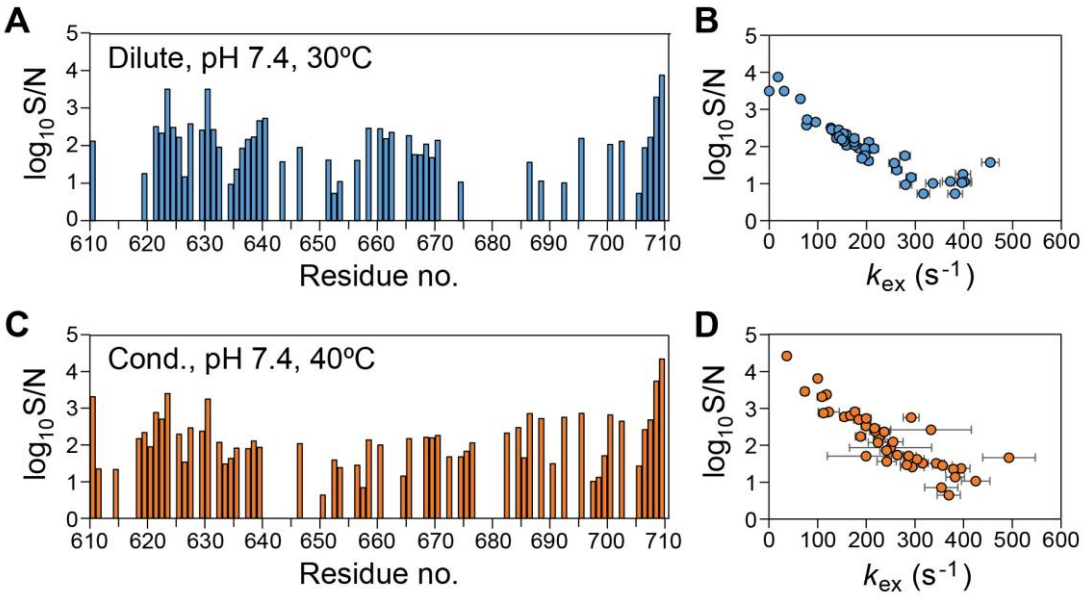

Figure S2. Signal-to-noise ratios of peaks in HNCO spectra are inversely correlated with k_{ex}. (A and C) Log_{10}(signal-to-noise; S/N) in cross polarization-enhanced HNCO spectra of CAPRIN1 (A) dilute phase, 30°C, 25 mM HEPES, pH 7.4, and (C) condensed phase, 40°C, 25 mM HEPES, pH 7.4, 100 mM NaCl. S/N values in (A) were obtained from analysis of an HNCO spectrum acquired with non-uniform sampling (14.5 hr), $t_{1,max}$ (^{13}CO) = 50 ms, $t_{2,max}$ (^{15}N) = 55 ms and in (C) from a uniformly sampled HNCO (1d 3 hr), $t_{1,max}$ = 35.6 ms, $t_{2,max}$ (^{15}N) = 35.1 ms. (B and D) Log_{10}S/N *vs* k_{ex} (k_{ex} obtained from SE_haCONHA experiments); large errors in chemical shifts and exchange parameters are obtained for residues with S/N values < 10. Errors in k_{ex} are indicated.

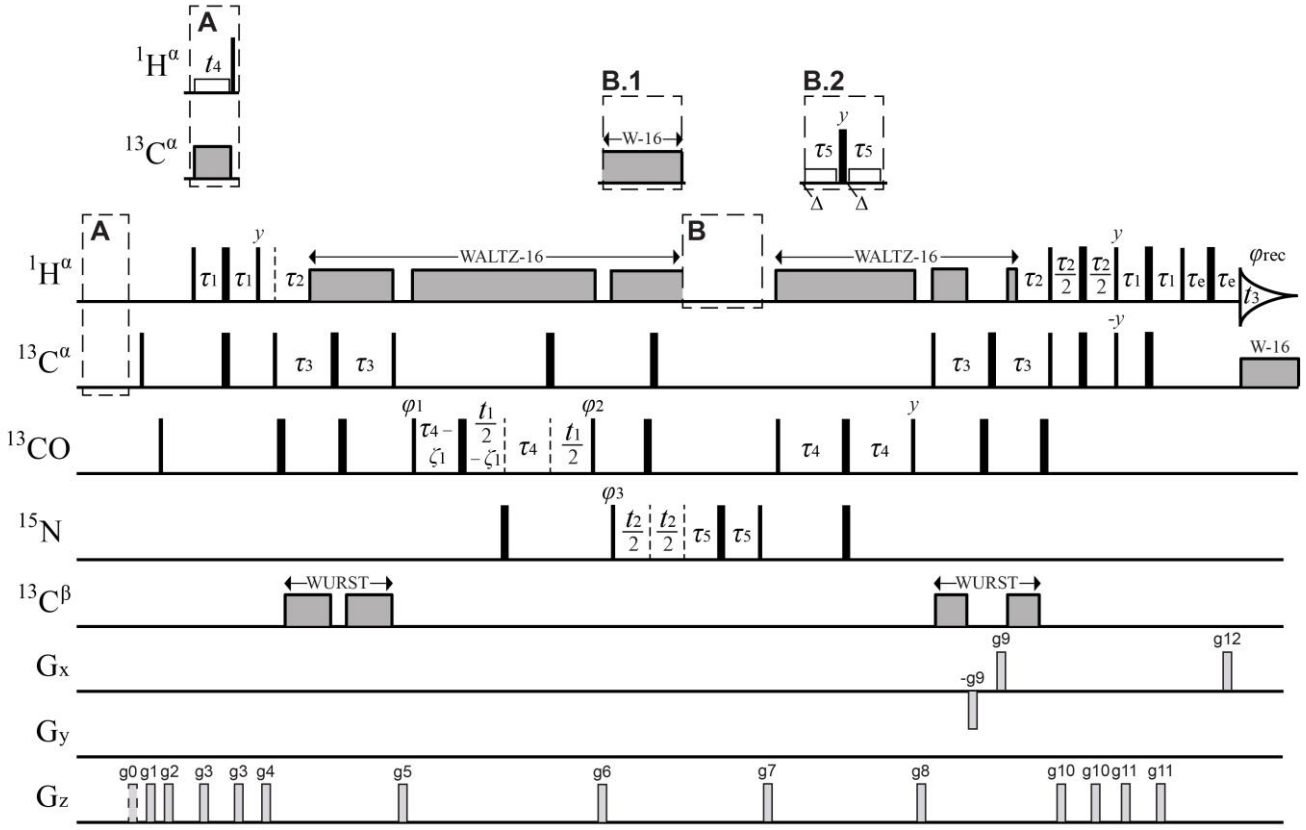

Figure S3. The SE_haCONHA experiment for indirect measurement of $^{1}H^{N}$ chemical shifts. The pulse scheme is closely related to the haCONHA sequence[2]; only the details that are unique to the spin-echo version of the experiment are described here and the interested reader is encouraged to consult reference 2 for other details. To obtain I/I_0 profiles, from which $^{1}H^{N}$ chemical shifts are fit, a set of 3D experiments is recorded with **A** omitted and **B**=**B.2**, with each data set recorded with a different Δ value (I). The spin echo delay, $2\tau_5$, is typically set to an odd multiple of $0.5/^{1}J_{HN}$, although this is not required. During each of the two τ_5 delays a weak ^{1}H cw field (generally 200-500 Hz) is applied. An additional 3D data set is recorded with **B**=**B.1** where ^{1}H WALTZ-16 decoupling is applied during the spin echo period (6.3 kHz field) to eliminate scalar coupled evolution of the ^{15}N magnetization (I_0). ^{13}CO chemical shift evolution during t_1 is acquired in a semi-constant time mode[16,17] that is implemented slightly differently than in the haCONHA experiment[2]. Here the delay ζ_i is defined as $\zeta_i = \{\tau_4/(n_i-1)\}\cdot(\varepsilon-1)$, where n_i is the total number of complex points in the time domain and ε is set to the current complex t_i point number, ranging from 1 to n_i. The phase cycle used is: $\varphi_1 = 2(x),2(-x)$; $\varphi_2 = y$-48.5°; $\varphi_3 = x,-x$; and $\varphi_{rec} = x,2(-x),x$. A phase change of -48.5° (600 MHz) is applied to φ_2 to correct the Bloch-Siegert shift[18] caused by application of the $^{13}C^{\alpha}$ π pulse during the t_1 period. In order to calibrate the weak ^{1}H B_1 field of strength ν_1 a nutation experiment, with **B**=**B.1** and scheme **A** included, is performed following the approach of Guenneugues *et al.*[19]. The ^{1}H carrier is placed on-resonance for an $^{1}H^{\alpha}$ peak of interest (preferably one of high intensity and well-resolved) and a 2D data set recorded by incrementing t_4

during which time the weak cw B_1 field that is to be calibrated is applied (t_4 increments of less than $0.5/\nu_1$). In addition, $^{13}C^{\alpha}$ decoupling is applied, on resonance for the $^{13}C^{\alpha}$ that is one-bond coupled to the $^{1}H^{\alpha}$ of interest, using a composite pulse, $90°_x$-$240°_y$-90°x, scheme[20] with a field of ~2 kHz. For each t_4 value a pair of FIDs is recorded, with and without the ^{1}H 90^o pulse that follows the ^{1}H cw field, to obtain quadrature in the indirect dimension[21]. The position of the peak in the F_1 dimension corresponds to ν_1. Gradients are applied with the following durations (ms) and strengths (in % maximum): g0: (1.0, 40%), g1: (0.5, 24%), g2: (1.0, 24%), g3: (0.256, 15%), g4: (1.0, 40%), g5: (1.25, 80%), g6: (1.5, 80%), g7: (0.9, 50%), g8: (1.0, 15%), g9: (0.512, 90%), g10: (0.4, 40%), g11: (0.3, 15%), g12: (0.256, 90.3%). The pulse scheme is available upon request.

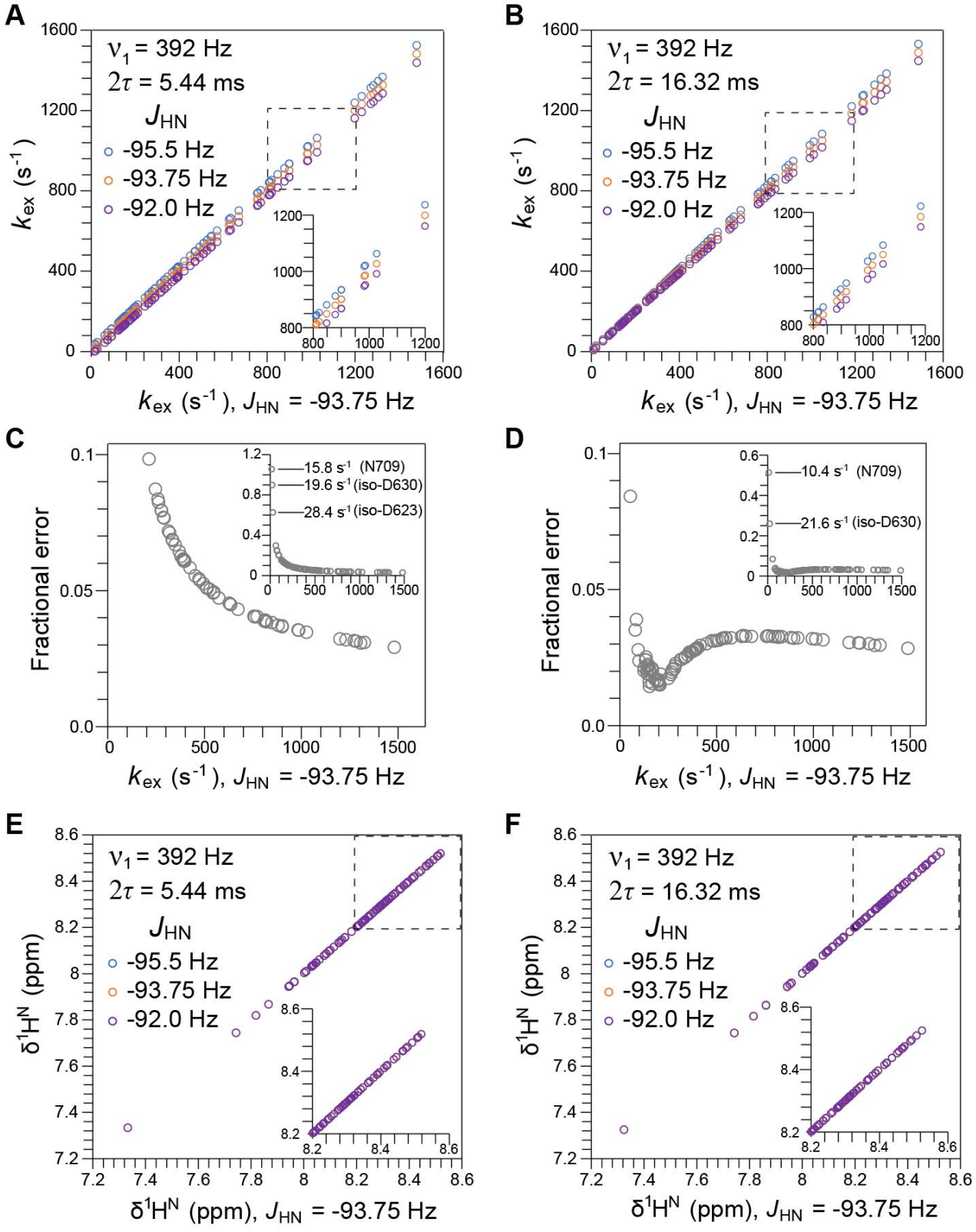

Figure S4. Small variation in $^1J_{HN}$ values have little effect on extracted $^1H^N$ chemical shifts and k_{ex} values. (A and B) Linear correlation plots of extracted k_{ex} values from fits of an experimental data set

recorded on a sample of dilute phase CAPRIN1, 25 mM HEPES, pH 7.4, 30°C, measured using 2τ values of 5.44 ms (A) and 16.32 ms (B). Data sets were analyzed separately by assuming three different $^1J_{HN}$ values of -95.5, -93.75, and -92.0 Hz (y-axis) and the resultant k_{ex} rates compared with those obtained when $^1J_{HN}$ = -93.75 Hz (x-axis). The range of $^1J_{HN}$ values considered here (-93.75±1.75 Hz) is slightly larger than the range of values in proteins, -93.7±1.1 Hz (see main text). Note that the extracted k_{ex} rates increase with the assumed $|^1J_{HN}|$ value; thus, if $^1J_{HN}$ used in the fits overestimates the correct coupling 'constant' then fitted k_{ex} values will be too large. The mean deviation in k_{ex} = <(k_{ex}(-95.5 Hz) – k_{ex}(-92.0 Hz))/2> is 25 s^{-1} and 13 s^{-1} in A and B, respectively. Insets show small, expanded regions of the main graphs. (C and D) Fractional error in k_{ex} *vs* k_{ex}, defined as (k_{ex}(-95.5 Hz) – k_{ex}(-92.0 Hz))/(2k_{ex}(-93.75 Hz) for 2τ = 5.44 ms (C) and 16.32 ms (D). Insets show the full range of k_{ex} values. Median fractional errors of 7% and 3% are obtained in (C) and (D), respectively, indicating that $2\tau \approx 1.5/^1J_{HN}$ is preferred over $2\tau \approx 0.5/^1J_{HN}$ with respect to errors associated with (small) variations in $^1J_{HN}$ values. (E and F) Linear correlation plots of extracted $^1H^N$ chemical shifts fitted with three different $^1J_{HN}$ values as above, for 2τ = 5.44 ms (E) and 16.32 ms (F). Note that the extracted shifts are invariant to the assumed $^1J_{HN}$ value.

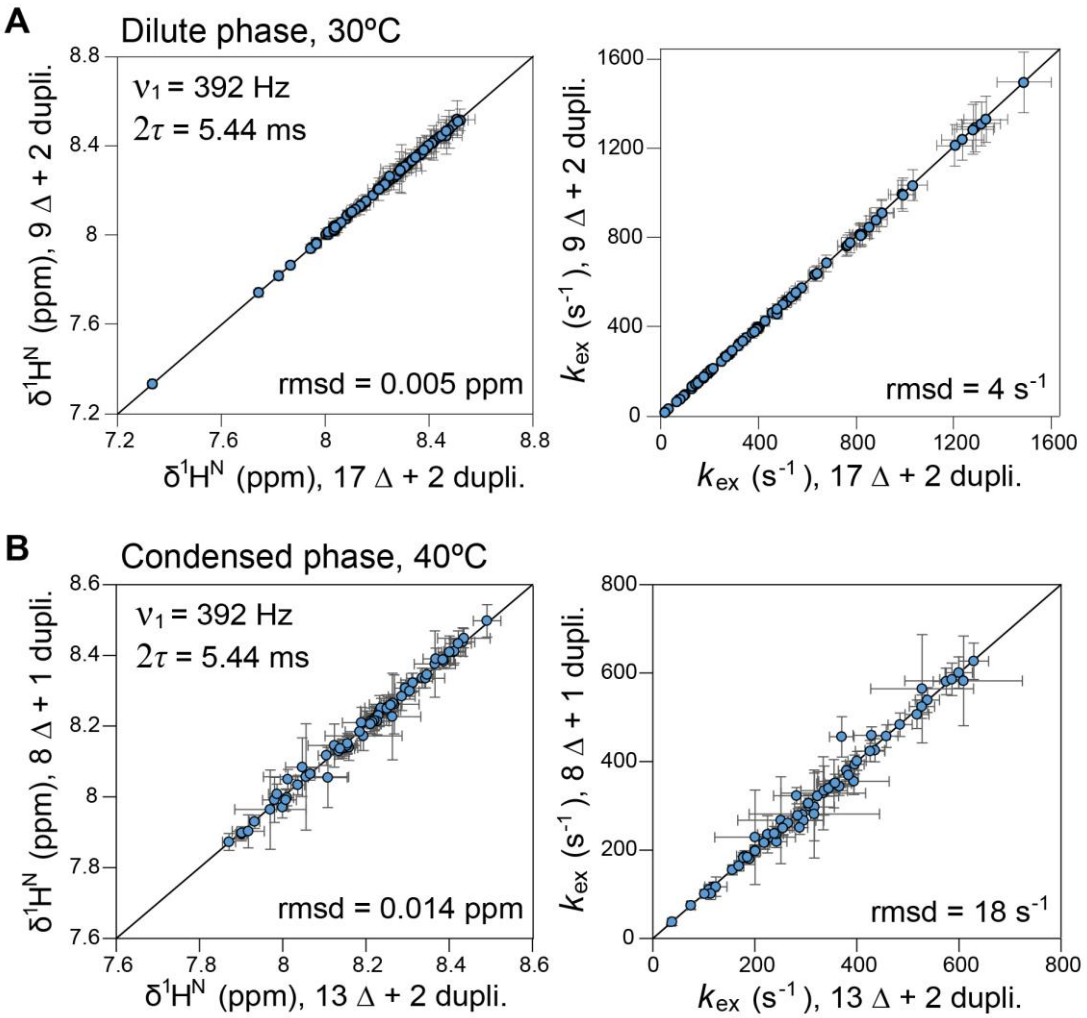

Figure S5. Robust parameters are obtained when only 50-60% of SE_haCONHA data is included in the fit. (A and B) Linear correlation plots of extracted $^{1}H^{N}$ chemical shift (left) or k_{ex} (right) values from analysis of a subset of the recorded Δ values for (A) dilute phase CAPRIN1, 25 mM HEPES, pH 7.4, 30°C or (B) condensed phase CAPRIN1, 25 mM NaPi, 100 mM NaCl, pH 7.4, 40°C. Values of Δ are separated by 150 Hz and 300 Hz for the larger and smaller data sets, respectively, in (A), and by 200 and 400 Hz, respectively, in (B). The total measurement times for the larger and smaller data sets are: (A) 19.5 hr and 11.7 hr, respectively; (B) 65.3 hr and 40.8 hr, respectively.

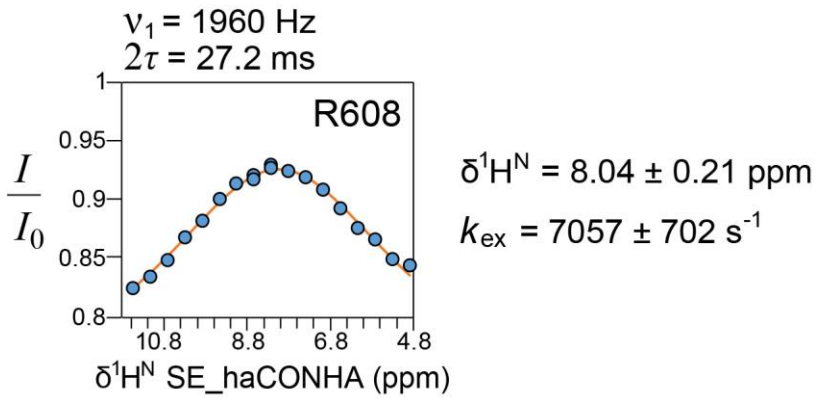

Figure S6. Measurement of $^{1}H^{N}$ chemical shift and k_{ex} for R608. As described in the text, the rapid amide proton exchange of R608 with water precluded measurement of its chemical shift using $2\tau \approx 0.5/^{1}J_{HN}$ and ν_1 = 392 Hz. In contrast, a broad but measurable I/I_0 profile was obtained using $2\tau \approx 2.5/^{1}J_{HN}$, ν_1 = 1960 Hz from which $\delta^{1}H^{N}$ and k_{ex} values could be obtained.

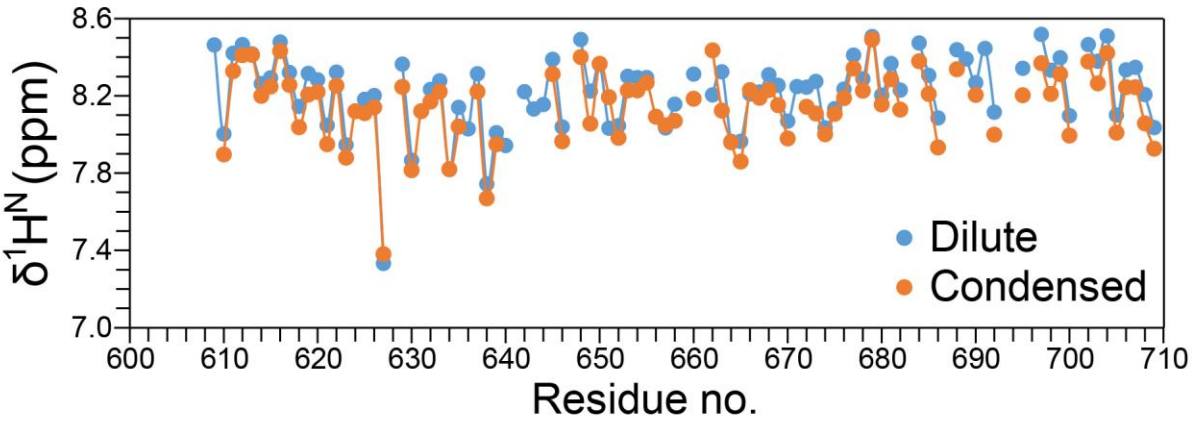

Figure S7. $^{1}H^{N}$ chemical shifts of dilute and condensed phase CAPRIN1. The $^{1}H^{N}$ chemical shifts of CAPRIN1 in dilute phase (25 mM HEPES, pH 7.4, 30°C, 87 residues) were determined from the SE_haCONHA experiment while those of the condensed phase (25 mM NaPi, 100mM NaCl, pH 7.4, 40°C, 81 residues) were obtained from analysis of both SE_haCONHA and HNCO experiments.

Table S1

Experiment[a]	t_{1max} (ms)	t_{2max} (ms)	t_{3max} (ms)	NS	Time (hr)	Remarks
Dilute CAPRIN1 (0.5 mM), 25 mM MES, pH 5.5						
CP-HISQC[b]	55	64		8	1	T = 30°C, d_1 (relaxation delay)= 2 s
HNCO[c]	60	55	64	4	2	T = 25°C, NUS = 5 %, d_1 = 2 s
SE_haCONHA	60	55	64	2	19.5	T = 25°C, NUS = 5 %, d_1 = 1 s, 2τ = 5.44 ms, ν_1 = 392 Hz, 17 Δ offsets + 2 duplicates
Dilute CAPRIN1 (0.7 mM), 25 mM HEPES, pH 7.4						
CP-HISQC[b]	55	64		8	1	T = 30°C, d_1 = 2 s
HNCO[c]	50	55	64	4	19.5	T = 30°C, NUS = 33 %, d_1 = 2 s
SE_haCONHA	60	55	64	2	19.5	T = 30°C, NUS = 5 %, d_1 = 1 s, 2τ = 5.44 ms, ν_1 = 392 Hz, 17 Δ offsets + 2 duplicates
SE_haCONHA	60	55	64	2	19.5	Same as above except for 2τ = 16.32 ms
SE_haCONHA	60	55	64	2	19.5	Same as above except for ν_1 = 196 Hz
SE_haCONHA	60	55	64	2	19.5	Same as above except for ν_1 = 530 Hz
Condensed CAPRIN1 (15 mM total protein, 2 mM ^{15}N,^{13}C-labeled protein), 25 mM NaPi, 100 mM NaCl, pH 7.4, T = 40°C						
HNCO[c]	37	41	64	8	65.8	d_1 = 2 s
SE_haCONHA	28	35	64	20	65.3	NUS = 7 %, d_1 = 1 s, 2τ = 5.44 ms, ν_1 = 392 Hz, 13 offsets + 2 duplicates

[a] t_{jmax} is the maximum acquisition time in the j dimension; NS is the number of transients averaged per FID and Time is the total measurement time for the data set.

[b] $^1H^N$-^{15}N HSQC scheme of Yuwen and Skrynnikov[3], optimized for studies of IDPs at high pH.

[c] HNCO scheme that includes elements from the CP-HISQC sequence[3] to optimize signal-to-noise in studies of IDPs.

Table S2

Residue	$^{1}H^{N}$ chemical shifts of Gly residues (ppm)	
	Dilute phase (pH 7.4, 30°C)	**Condensed phase (pH 7.4, 40°C)[a]**
G609	8.46	
G613	8.42	8.41
G614	8.26	8.20
G617	8.32	8.26
G620	8.28	8.22
G627	7.33	7.38
G634	7.82	7.82
G635	8.14	8.04
G638	7.74	7.67
G650	8.36	8.37
G664	7.96	7.96
G669	8.26	8.15
G677	8.41	8.34
G679	8.51	8.49
G682	8.23	8.13
G685	8.31	8.21
G689	8.39	
G691	8.45	
G692	8.11	8.00
G699	8.40	8.31

[a]Not all $^{1}H^{N}$ chemical shifts in the condensed phase could be obtained.

References

(1) Kim, T. H.; Tsang, B.; Vernon, R. M.; Sonenberg, N.; Kay, L. E.; Forman-Kay, J. D. Phospho-Dependent Phase Separation of FMRP and CAPRIN1 Recapitulates Regulation of Translation and Deadenylation. *Science* **2019**, *365* (6455), 825–829. https://doi.org/10.1126/science.aax4240.

(2) Wong, L. E.; Kim, T. H.; Muhandiram, D. R.; Forman-Kay, J. D.; Kay, L. E. NMR Experiments for Studies of Dilute and Condensed Protein Phases: Application to the Phase-Separating Protein CAPRIN1. *J. Am. Chem. Soc.* **2020**. https://doi.org/10.1021/jacs.9b12208.

(3) Yuwen, T.; Skrynnikov, N. R. CP-HISQC: A Better Version of HSQC Experiment for Intrinsically Disordered Proteins under Physiological Conditions. *J. Biomol. NMR* **2014**, *58* (3), 175–192. https://doi.org/10.1007/s10858-014-9815-5.

(4) Jaravine, V.; Ibraghimov, I.; Orekhov, V. Y. Removal of a Time Barrier for High-Resolution Multidimensional NMR Spectroscopy. *Nat. Methods* **2006**, *3* (8), 605–607. https://doi.org/10.1038/nmeth900.

(5) Stanek, J.; Koźmiński, W. Iterative Algorithm of Discrete Fourier Transform for Processing Randomly Sampled NMR Data Sets. *J. Biomol. NMR* **2010**, *47* (1), 65–77. https://doi.org/10.1007/s10858-010-9411-2.

(6) Hyberts, S. G.; Arthanari, H.; Wagner, G. *Applications of Non-Uniform Sampling and Processing*; Billeter,Martin; Orekhov, V., Ed.; Springer, Berlin, Heidelberg, 2012; Vol. 316. https://doi.org/10.1007/128_2011_187.

(7) Hyberts, S. G.; Takeuchi, K.; Wagner, G. Poisson-Gap Sampling and Forward Maximum Entropy Reconstruction for Enhancing the Resolution and Sensitivity of Protein NMR Data. *J. Am. Chem. Soc.* **2010**, *132* (7), 2145–2147. https://doi.org/10.1021/ja908004w.

(8) Ying, J.; Delaglio, F.; Torchia, D. A.; Bax, A. Sparse Multidimensional Iterative Lineshape-Enhanced (SMILE) Reconstruction of Both Non-Uniformly Sampled and Conventional NMR Data. *J. Biomol. NMR* **2017**, *68* (2), 101–118. https://doi.org/10.1007/s10858-016-0072-7.

(9) Delaglio, F.; Grzesiek, S.; Vuister, G. W.; Zhu, G.; Pfeifer, J.; Bax, A. NMRPipe: A Multidimensional Spectral Processing System Based on UNIX Pipes. *J. Biomol. NMR* **1995**, *6* (3), 277–293. https://doi.org/10.1007/BF00197809.

(10) Long, D.; Delaglio, F.; Sekhar, A.; Kay, L. E. Probing Invisible, Excited Protein States by Non-Uniformly Sampled Pseudo-4D CEST Spectroscopy. *Angew. Chemie - Int. Ed.* **2015**, *54* (36), 10507–10511. https://doi.org/10.1002/anie.201504070.

(11) Yang, D.; Venters, R. A.; Mueller, G. A.; Choy, W. Y.; Kay, L. E. TROSY-Based HNCO Pulse Sequences for the Measurement of (1)HN-(15)N, (15)N-(13)CO, (1)HN-(13)CO, (13)CO-(13)C(α) and (1)HN-(13)C(α) Dipolar Couplings in (15)N, (13)C, (2)H-Labeled Proteins. *J. Biomol. NMR* **1999**, *14* (4), 333–343. https://doi.org/10.1023/A:1008314803561.

(12) Kateb, F.; Pelupessy, P.; Bodenhausen, G. Measuring Fast Hydrogen Exchange Rates by NMR Spectroscopy. *J. Magn. Reson.* **2007**, *184* (1), 108–113. https://doi.org/10.1016/j.jmr.2006.09.022.

(13) Sehgal, A. A.; Duma, L.; Bodenhausen, G.; Pelupessy, P. Fast Proton Exchange in Histidine: Measurement of Rate Constants through Indirect Detection by NMR Spectroscopy. *Chem. - A Eur. J.* **2014**, *20* (21), 6332–6338. https://doi.org/10.1002/chem.201304992.

(14) Skrynnikov, N. R.; Ernst, R. R. Detection of Intermolecular Chemical Exchange through Decorrelation of Two-Spin Order. *J. Magn. Reson.* **1999**, *137* (1), 276–280. https://doi.org/10.1006/jmre.1998.1666.

(15) Press, William H.; Flannery, Brian P.; Teukolsky, Saul A.; Vetterling, W. T. *Numerical Recipes in C: The Art of Scientific Computing*, 2nd Ed.; Cambridge University Press, 1992.

(16) Grzesiek, S.; Anglister, J.; Bax, A. Correlation of Backbone Amide and Aliphatic Side-Chain Resonances in 13C/15N-Enriched Proteins by Isotropic Mixing of 13C Magnetization. *J. Magn. Reson. Ser. B* **1993**, *101* (1), 114–119. https://doi.org/10.1006/jmrb.1993.1019.

(17) Logan, T. M.; Olejniczak, E. T.; Xu, R. X.; Fesik, S. W. A General Method for Assigning NMR Spectra of Denatured Proteins Using 3D HC(CO)NH-TOCSY Triple Resonance Experiments. *J. Biomol. NMR* **1993**, *3* (2), 225–231. https://doi.org/10.1007/BF00178264.

(18) Freeman, R. *A Handbook of Nuclear Magnetic Resonance*; Longman Scientific & Technical, 1987.

(19) Guenneugues, M.; Berthault, P.; Desvaux, H. A Method for Determining B 1 Field Inhomogeneity. Are the Biases Assumed in Heteronuclear Relaxation Experiments Usually Underestimated? *J. Magn. Reson.* **1999**, *136* (1), 118–126. https://doi.org/10.1006/jmre.1998.1590.

(20) Levitt, M. H. Symmetrical Composite Pulse Sequences for NMR Population Inversion. II. Compensation of Resonance Offset. *J. Magn. Reson.* **1982**, *50* (1), 95–110. https://doi.org/10.1016/0022-2364(82)90035-X.

(21) Yuwen, T.; Bah, A.; Brady, J. P.; Ferrage, F.; Bouvignies, G.; Kay, L. E. Measuring Solvent Hydrogen Exchange Rates by Multifrequency Excitation 15 N CEST: Application to Protein Phase Separation. *J. Phys. Chem. B* **2018**, *122* (49), 11206–11217. https://doi.org/10.1021/acs.jpcb.8b06820.

/* hacacon_HN_lek_600_cp_3D

Use this sequence for 3Ds that allows running of NUS with frequencies
of 1H irradiation set internally

1Ha(t1) > 13Ca to 13CO (58 ppm) > 13CO (176 ppm, t1) to 15N (t2)
> CEST-like to get 1HN shift > CO > Ca > Ha (t3)

3D pulse scheme to record (CO,N,Ha) with modulation of intensity according to
to HN chemical shift; need to record a set of N 3D consecutively with different
HN rf frequencies using NUS

a: 13C carrier at 58 ppm
pwc90 D/sq(15) where D = 118 ppm (on res), p24, pl24
pwc180 D/sq(3) where D = 118 ppm (on res), p25, pl25
pwc180:sp25 D/sq(3) where D = 118 ppm (off res, using pwco180b:sp25, + shift)
p25, sp25

using 13Cb decoupling with pl27 and onepulse.sp27

b: 13C carrier at 176 ppm
pwc90 D/sq(15) where D = 118 ppm (on res), p24, pl24
pwc180 D/sq(3) where D = 118 ppm (on res), p25, pl25
pwc180:sp30 D/sq(3) where D = 118 ppm (off res, using :pwca180c:sp30 , - shift)
p25,sp30

To be used in phase separated or IDP samples to generate CO,N type spectra with higher s/n than CO detect
Uses shared constant time in CO

Written by LEK on Nov 13, 2018

Modified by LEK on Nov 19,20, 2018 to ensure that water is dephased and to add bipolars between the 15N t2 period that helps. Tried mess purge at end but this is less effective than 90 180 90

Decoupling of amides cannot be achieved with 1H 180 in middle of 15N t2. This causes rapid decay of 15N signal because Nx > 2NyIz and the 2NyIz decause quickly due to exchange with water

Found that making CO inphase with respect to 13Ca before 15N t2 and then antiphase with 13Ca during
the subsequent 2T element losses about 10% of signal. Presumably the Ca 180s hit the Cb, Cg that are coupled to CO such that there is dephasing for the 10 ms due to couplings with them - not sure

Uses phase ph10:r to compensate for BS effect rather than an additional pulse - at 600 MHz use 48.5o (check phcor) should be 51o

Modified by LEK on Jan 11, 2019 to include N_180 that places an 15N 180 in the middle of t2
for 2D (CO,Ha)

Modified by LEK on March 19, 2019 to include option for gradient transfer
Water suppression is better but there is a sensitivity loss of 15% or so with setup for AX spin systems

Additional 8% loss with taub = 1.15ms and 32% loss in AX2 spin system sensitivity (GLY)
-Dgd_sel

Modified by LEK on May 12, 2019 to modify the way the shared CT in CO is done; now done using the method of Bax

Modified by LEK on Sept 25, 2019 to allow internal entry of frequencies; set l15 to be number of frequencies
Set TD2 to be l15*(total number of points in 15N dimension)

Modified by LEK on Oct 2, 2019 to calibrate about a 1 ms pulse on 1H (p11) at a power level pl11 to be used
to get the weak B1 field

Modified by LEK on Oct 31, 2019 to enable callibration of B1 field by nutation: SET -Dcal_HB1 and -DN_flg
Set F2 to be number of R+I points, and to 1H (does not require external list of delay values but uses 'normal' acquisition in the calibration dimension - set sw in F2 properly

*/

```
#include <Avance.incl>
#include <Grad.incl>
#include <Delay.incl>

;Define phases
#define zero ph=0.0
#define one ph=90.0
#define two ph=180.0
#define three ph=270.0

;Define Pulses
define pulse pwh
      "pwh=p1"

define pulse pwh_soft
      "pwh_soft=p13"

define pulse pwn
      "pwn=p3"

;Carbon pulses when 13C carrier is at 58ppm/176ppm:
define pulse pwc90
      "pwc90=p24"
define pulse pwc180
      "pwc180=p25"

define pulse dly_pg1
  "dly_pg1 = p15"
define pulse dly_pg2
  "dly_pg2 = p16"
```

```
;Define delays
"d11=30m"

"in0=inf1/2"   ; 1H dimension
"in10=inf2/2"  ; 15N dimension

"TAU2 = 0.2u"

define delay taua
      "taua = d20"      ; < 1/4JCH ~ 1.8 ms

define delay taub
      "taub = d21"     ;  1/4JCH (exactly 1.8 ms)

define delay tauc
      "tauc = d22"       ; ~ 1/4JCaCO ~ 9 ms ARRAY with Cb dec

define delay taue
      "taue = d24"      ; ~ 1/4JNCO , ~ 16 ms

define delay hscuba
     "hscuba = 30m"

;Define flags
;define f1180  ; set zgoptns -Df1180

#ifdef f1180
 "d0= (in0/2)"   ; CO evolution f1180 y or n
#else
 "d0=0.2u"
#endif

#ifdef f2180
 "d10= (in10/2)"   ; N15 evolution f1180 y
#else
 "d10=0.2u"
#endif

;aqseq 321     ; Determines the order of acquisition when 'mc' macro is used.

#ifndef oneDarray
define loopcounter ni
      " ni= td1/2"
#endif

define loopcounter zetacount
define delay zetaB
define delay zetaB2

/* Assign cnsts to check validity of parameter range */
#ifdef fsat
  "cnst10 = plw10" ; tsatpwr - set max at 0.8 W
```

```
#endif

  "cnst12=plw12" ; tpwrml - set max at 2 W 1H waltz decoupling

  "cnst22=plw21" ; power level for 13C decoupling
  "cnst24=plw24" ; C 90 D/sq(15) set max at 11.0W
  "cnst25=plw25" ; C 180 D/sq(3) set max at 52.0W
#ifdef cal_HB1
  "cnst26=plw26" ; power level for 13C decoupling during nutation
#endif
  "cnst27=plw27" ; Cb decoupling - set max at 2.0W
  "cnst28=spw25" ; C 180 D/sq(3) set max at 52.0W
  "cnst29=spw30" ; C 180 D/sq(3) - set max at 52.0W
  "cnst31=plw31" ; dpwr2 - set max at 6W

#ifndef gd_sel
"acqt0 = -pwh*2.0/PI" ; assumes regular INEPT TRANSFER BACK
#else
"acqt0 = 0.0u" ; enhanced sensitivity TRANSER BACK
baseopt_echo
#endif

"d27=0.2u"
"d30=0.0u"

/* MAKE SURE FORMAT IS = { A B C } */

define list<frequency> H1_offset = { 20000 780 930 1080 1230 1380 1530 1680 1830 1980 2130 2280
2430 2580 2730 2880 3030 3180 780 1980 }  /* CHANGE */
"l15=20"  /* CHANGE */

#ifndef N_flg
"p18 = 1s/(4.0*cnst16)"    ; cnst16 in Hz is the B1 field
"plw18 = plw11*(p11)*(p11)/((p18)*(p18))"    ; plw11 is the power level for the approx 1 ms pulse to
calibrate weak B1 field
"cnst18 = plw18"   ; power level for weak amide B1 field
#endif

/* BEGIN ACTUAL PULSE SEQUENCE */

"l0=0" ; frequency counter

#ifdef cal_HB1
"p18 = 1s/(4.0*cnst16)"    ; cnst16 in Hz is the B1 field
"plw18 = plw11*(p11)*(p11)/((p18)*(p18))"    ; plw11 is the power level for the approx 1 ms pulse to
calibrate weak B1 field
"cnst18 = plw18"   ; power level for weak amide B1 field
"l30=0"
#endif

1 ze
```

```
; check validity of parameters

if "aq > 0.07s" {
   2u
   print "error: acq time is too long; < 70 ms"
   goto HaltAcqu
}

#ifdef fsat
   if "cnst10 > 0.5"
  {
   2u
   print "error: tsatpwr, pl10 is incorrect"
   goto HaltAcqu
  }
#endif

  if "cnst12 > 2.0"
  {
   2u
   print "error: 1H waltz16 decoupling is too large  < 2W"
   goto HaltAcqu
  }

  if "cnst16 > 2000"
  {
   2u
   print "error: Weak 1H B1 field is too large < 2000 Hz"
   goto HaltAcqu
  }

  if "cnst24 > 12.0"
  {
   2u
   print "error: pl24 too larg"
   goto HaltAcqu
  }

  if "cnst25 > 60.0"
  {
   2u
   print "error: pl25 too large"
   goto HaltAcqu
  }

#ifdef cal_HB1
  if "cnst26 > 2.0"
  {
   2u
   print "error: pl26 too large (13C decoupling during nutation"
   goto HaltAcqu
  }
```

```
#endif

  if "cnst28 > 60.0"
  {
   2u
   print "error: spw25 too large"
   goto HaltAcqu
  }

  if "cnst29 > 60.0"
  {
   2u
   print "error: spw30 too large"
   goto HaltAcqu
  }

  if "cnst27 > 0.5"
  {
   2u
   print "error: power for Cb decoupling is too high"
   goto HaltAcqu
  }

  if "cnst22 > 2.0"
  {
   2u
   print "error: pl21 C decoupling is too large"
   goto HaltAcqu
  }

  if "cnst31 > 0.0"
  {
   2u
   print "error: pl31 incorrect, there is no decoupling on 15N"
   goto HaltAcqu
  }

  if "dly_pg1 > 9.0m"
  {
   2u
   print "error: dly_pg1 is too long"
   goto HaltAcqu
  }

  if "dly_pg2 > 9.0m"
  {
   2u
   print "error: dly_pg2 is too long"
   goto HaltAcqu
  }

#ifndef oneDarray
```

```
if "ni>1" {
  "d27 = in0 - (taue - 2.0u)/(ni-1)"
  if "d27 < 0.2u"
  {
   2u
   print "error: Bax method substracts more than 1/2sw1 each time"
   goto HaltAcqu
  }
}
#endif

2 d11 do:f2

2u pl11:f1

#ifdef mess_flg
 2u pl12:f1        ;   dly 2u, set power to pl12
 (dly_pg1 zero):f1   ;   2ms
 2u                ;   dly 2u
 (dly_pg2 one):f1    ;   3ms

  20u UNBLKGRAD

  2u
  (p59:gp9)
  d16
  20u BLKGRAD
#endif

  2u pl1:f1       ; set power pl1 for 1H hard pulses
  2u pl24:f2      ; set power pl24 for 13C hard pulses
  2u pl3:f3       ; set power pl3 for 15N hard pulses

#ifdef fsat                       ; zgoptn -Dfsat
  4u pl10:f1                       ; power(tsatpwr) for presaturation
  d1 cw:f1 zero                      ; Hcw(d1)x
  4u do:f1                        ; cw off
  2u pl1:f1                       ; power(tpwr)

#ifdef fscuba                 /* Scuba pulse sequence */
   hscuba                     ; delay(hscuba)
    (pwh zero):f1                ; H 90x180y90x
    (pwh*2 one):f1
    (pwh zero):f1
   hscuba                      ; delay(hscuba)
#endif                       /* end fscuba */

#else                        /* if fsat is no */
 2u pl1:f1                     ; power(tpwr)
 d1                          ; delay(d1)
#endif                        /* end if fsat */
```

```
  2u fq=0:f2                        ; 13C SFO2 @ 58ppm

  2u pl1:f1

  20u UNBLKGRAD

; ensure magnetization originates on 1H not on C or N

  (pwc90 ph26):f2

  2u
  (p50:gp0)
  d16

  2u fq=cnst21:f2           ; jump to CO, apply purge

  (pwc90 ph26):f2

  2u
  (p50*2.0:gp0)
  d16

  2u fq=0:f2              ; return to Ca

; This is the real start

#ifndef oneDarray

; first generate Bax/Logan for t1
  "DELTA = taue - 2u - 2u"

 if "ni > 1" {
    "zetaB = DELTA/(ni-1)"
}
else {
    "zetaB=0.1u"
}
0.2u

if " zetaB < 0.1u "
  {
   2u
   print "error: problem with zetaB for t1"
   goto HaltAcqu
  }

#ifdef f1180
   "d30 = d0 - in0/2"
   "zetacount = trunc(d30/in0 + 0.4)"
   "zetaB2 = zetaB*zetacount"
#else
   "d30 = d0 - 0.2u"
```

```
   "zetacount = trunc(d30/in0 + 0.4)"
   "zetaB2 = zetaB*zetacount"
#endif
; end of bax logan setup
#else
 "zetaB2 = 0.1u"
#endif

#ifdef cal_HB1    /* calibration of 1H B1 field */
"DELTA = d10*2"

 if "DELTA > 60m" {
    2u
    print "error: time_cal (evolution time) during B1 calib is too long"
    goto HaltAcqu
}
0.2u

2u pl26:f2              ; adjust power for 13C cw decoupling
4u fq=cnst23:f2         ; jump 13C carrier to on resonance for 13C that is coupled to 1H of interest
(2u cpds5 ph26):f2      ; 90x240y90x decoupling

2u pl18:f1              ; turn 1H power for nutation
2u fq=cnst11:f1         ; jump to center of 1Ha peak
(DELTA cw ph26):f1
2u do:f1
2u pl1:f1

if "l30%2 == 1" {
(pwh ph26):f1           ; to obtain quadrature
}

2u do:f2

4u fq=0:f1          ; jump to water
4u fq=0:f2          ; jump to Ca

  2u
  p52:gp2
  d16
#endif

  (pwh ph26):f1

  2u
  p51:gp1
  d16

  "DELTA = taua - 2.0u - p51 - d16 - 2u"
   DELTA

  2u pl25:f2
```

```
  (center (pwh*2.0 ph26):f1 (pwc180 ph26):f2)

  "DELTA = taua - 2.0u - p51 - d16"
   DELTA

  2u
  p51:gp1
  d16

  (pwh ph27):f1

; no gradient if one wishes to preserve water

  2u
  p52:gp2
  d16

  2u pl24:f2
  (pwc90 ph1):f2
   2u

  (pwc180:sp25 ph26):f2                ; shaped CO180x Bloch Seigert

  2u pl27:f2                          ; power for Cb dec
  (2u cpds7 ph26):f2                   ; Cb dec ON

  "DELTA = taub*2.0 - 2u - pwc180 - 2u - 2u"
   DELTA

; start 1H decoupling

   2u pl12:f1                         ; power for 1H dec do not use 90x pulse on 1H as water along y
   (2u cpds1 ph27):f1                   ; waltz16y ON

  "DELTA = tauc - taub*2.0 - 2u - 2u - 2u - 2u"
   DELTA                               ; dly 1/4JCaCO

/* Turn off 13Cb decoupling */
  2u do:f2                             ; Cb dec off
  2u pl25:f2                           ; power for Ca/CO 180b

  (pwc180 ph26):f2                     ; Ca180(zero)
  2u
  (pwc180:sp25 ph26):f2                ; shaped CO180x

/* Turn on 13Cb decoup */
  2u pl27:f2                           ; power for Cb decoupling
  (2u cpds7 ph26):f2                   ; Cb dec ON

  "DELTA = tauc - 2u - pwc180 - 2u - 2u - 2u - 2u"
   DELTA                               ; dly 1/4JCaCO
```

```
  2u do:f2                                ; Cb dec off
  2u pl24:f2                               ; power for Ca 90b
  (pwc90 ph26):f2

; turn off 1H decoupling and apply gradient
  2u do:f1
  p56:gp6
  d16

; turn 1H decoupling back on after p56 gradient

  (2u cpds1 ph27):f1                       ; waltz16y ON

/* now move the 13C carrier to CO */

  2u
  20u fq=cnst21:f2   ; jump from 58 to 176 ppm

  2u pl24:f2
  (pwc90 ph2):f2

  "DELTA = taue - zetaB2 - 2.0u"
   DELTA

   2u pl25:f2
   (pwc180 ph26):f2

  "DELTA = d0 - zetaB2"
   DELTA

   (pwn*2.0 ph5):f3

  "DELTA = taue - pwn*2.0 - pwc180 - 2u"
   DELTA

  (pwc180:sp30 ph26):f2       ; ca pulse while sitting on co
  2u pl24:f2

  d0

  (pwc90 ph10:r):f2

2u pl25:f2

; turn off decoupling apply gradient turn back on

  2u do:f1

  2u
  p54:gp4
  d16
```

```
  (2u cpds1 ph26):f1

  (pwn ph3):f3

#ifndef N_flg
  "TAU3=larger(d10-pwc180-1u,TAU2)"

  TAU3

  (pwc180 ph26):f2
  2u
  (pwc180:sp30 ph26):f2

  TAU3

; now commence the 15N spin echo period

if "l0 %l15 == 0" {
  "DELTA = pwh_soft"
  1.2u
  DELTA
  (pwn*2 ph26):f3
  DELTA
  1u do:f1
}
else {
  1u do:f1
  1u pl18:f1
  "H1_offset.idx = l0"
  2u fq=H1_offset:f1
  (pwh_soft ph26):f1
  1u pl1:f1
  2u fq=0:f1
  (center (pwh*2.0 ph27):f1 (pwn*2 ph26):f3)
  2u fq=H1_offset:f1
  1u pl18:f1
  (pwh_soft ph26):f1
  3.8u
}
0.2u

#else
  1u
  (pwn*2.0 ph26):f3
  1u do:f1
#endif

  (pwn ph26):f3

  2u pl12:f1
  2u fq=0:f1
```

```
  2u
  p55:gp5
  d16

  (2u cpds1 ph27):f1

  2u pl24:f2
  (pwc90 ph26):f2
  2u pl25:f2

  "DELTA = taue - 2u"
   DELTA

  (center (pwc180 ph26):f2 (pwn*2 ph26):f3)

   DELTA

  2u pl24:f2
  (pwc90 ph27):f2

  10u fq=0:f2   ; jump carrier back to Ca

; first turn off 1H decopuling
  2u do:f1                              ; H dec off

#ifndef gd_sel
 2u pl12:f1        ;   dly 2u, set power to pl12
 (dly_pg1 zero):f1   ;   2ms
 2u                ;   dly 2u
 (dly_pg2 one):f1    ;   3ms
#endif

  2u
  p60:gp10
  d16

; now turn back on 1H decoupling
   2u pl12:f1                           ; power for 1H dec
   (2u cpds1 ph27):f1                        ; waltz16y ON

; transfer back from CaCO to Ca

#ifndef gd_sel

  (pwc90 ph26):f2

/* Turn on 13Cb decoup */
  2u pl27:f2                            ; power for Cb decoupling
  (2u cpds7 ph26):f2                        ; Cb dec ON

  "DELTA = tauc  - 2u - 2u - 2u - pwc180 - 2u"
   DELTA                                ; dly 1/4JCaCO
```

```
/* Turn off 13Cb decoupling */
 2u do:f2                                ; Cb dec off

 (pwc180:sp25 ph26):f2                   ; shaped CO180x
 2u pl25:f2
 (pwc180 ph26):f2                        ; Ca180(zero)

 2u pl27:f2                              ; power for Cb dec
 (2u cpds7 ph26):f2                      ; Cb dec ON

 "DELTA = tauc - taub*2.0 - 2u - 2u - 2u"
  DELTA                                  ; dly 1/4JCaCO

 /* Turn OFF 1H decoupling */
 2u do:f1                                ; H dec off

 "DELTA = taub*2 - 2u - pwc180 - 2u"
  DELTA

 2u do:f2

 (pwc180:sp25 ph26):f2                   ; shaped CO180x Bloch Seigert

 2u pl24:f2

 (pwc90 ph26):f2

2u pl1:f1         ;   set power to high power

 2u
 p57:gp7
 d16

 (pwh ph26):f1

 2u
 p58:gp8
 d16

 "DELTA = taua - 2.0u - p58 - d16 - 2u"
  DELTA

 2u pl25:f2
 (center (pwh*2.0 ph26):f1 (pwc180 ph26):f2)

 "DELTA = taua - 2.0u - p58 - d16 - 4u - 2u - 2u"
  DELTA

 2u
 p58:gp8
 d16
```

```
  4u BLKGRAD                          ; Blank gradients
  2u pl21:f2
  2u pl31:f3

  (pwh ph26):f1

#else

  (pwc90 ph26):f2

/* Turn on 13Cb decoup */
  2u pl27:f2                          ; power for Cb decoupling
  (2u cpds7 ph26):f2                    ; Cb dec ON

  "DELTA = tauc  - 2u - 2u - 2u - 2u - p41 - d16 - pwc180 - 2u"
   DELTA                              ; dly 1/4JCaCO

/* Turn off 13Cb decoupling */
  2u do:f2
  2u do:f1
  p41:gp14*-1.0                ; coherence transfer selection
  d16

  (pwc180:sp25 ph26):f2                 ; shaped CO180x
  2u pl25:f2
  (pwc180 ph26):f2                    ; Ca180(zero)

  2u
  p41:gp14                  ; coherence transfer selection
  d16

  (2u cpds1 ph27):f1                    ; waltz16y ON
   2u pl27:f2                       ; power for Cb dec
  (2u cpds7 ph26):f2                    ; Cb dec ON

  "DELTA = tauc - 2u - p41 - d16 - taub*2.0 - 2u - 2u - 2u - 2u"
   DELTA                              ; dly 1/4JCaCO

  /* Turn OFF 1H decoupling */
  2u do:f1                          ; H dec off

  "DELTA = taub*2 - 2u - 2u - pwc180 - 2u"
   DELTA

  2u do:f2
  2u pl1:f1

  (pwc180:sp25 ph26):f2                 ; shaped CO180x Bloch Seigert

  2u pl24:f2
  (center(pwh ph26):f1 (pwc90 ph26):f2)
```

```
2u
p42:gp15
d16

"DELTA = taub - 2.0u - p42 - d16 - 2u"
 DELTA

2u pl25:f2
(center (pwh*2.0 ph26):f1 (pwc180 ph26):f2)

"DELTA = taub - 2.0u - p42 - d16 - 2u"
 DELTA

2u
p42:gp15
d16

2u pl24:f2
(center(pwh ph27):f1 (pwc90 ph29):f2)

2u
p43:gp16
d16

"DELTA = taua - (pwc90-pwh)*0.5 - 2.0u - p43 - d16 - 2u"
 DELTA

2u pl25:f2
(center (pwh*2.0 ph26):f1 (pwc180 ph26):f2)

"DELTA = taua - 2.0u - p43 - d16"
 DELTA

2u
p43:gp16
d16

(pwh ph26):f1

"DELTA = 2u + p44 + d16 + 4u + 2u + 2u + de - pwh*2.0/PI"
 DELTA

(pwh*2 ph26):f1

2u
p44:gp17
d16

4u BLKGRAD                    ; Blank gradients
2u pl21:f2
2u pl31:f3
```

```
#endif

  go=2 ph31 cpds2:f2
  d11 do:f2 mc #0 to 2

#ifdef cal_HB1
  F2PH(calclc(l30,1), caldel(d10,+in10))
#else
  F2I(iu0,l15)   ; l15 is the number of frequencies
  F2PH(calph(ph3, +90) , calph(ph3, +180) & calph(ph31, +180) & caldel(d10, +in10))
#endif
  F1PH(calph(ph2, +90) , caldel(d0, +in0))

HaltAcqu, 1m
exit

ph1=0 0 0 0 2 2 2 2
ph2=0 0 2 2
ph3= 0 2
ph5=0
ph10=1
ph31=0 2 2 0 2 0 0 2
ph26=0
ph27=1
ph28=2
ph29=3

;cnst11 : freq difference in Hz between o1 and position of nutation (position of nutation - o1)
;cnst12 : power level for 1H waltz decoupling
;cnst16:  1H weak B1 field in Hz < 500 Hz
;cnst18:  power level for 1H weak B1 field in W
;cnst19:  frequency in Hz from o1 where weak 1H B1 is applied
;cnst21 : (176-58) ppm offset in Hz
;cnst23 : freq difference in Hz between o2 and 13C decoupling during 1H nutation (position of nutation
- o2)
;cnst24 : power level for 13C 90
;cnst25 : power level for 13C 180
;cnst26 : power level for 13C decoupling during nutation - can be same as decoupling during acq
;cnst27 : power level for 13Cb decoupling
;cnst22 : power level for 13C decoupling
;cnst31 : power level for 15N decoupling
;pl1 : tpwr - power level for pwh
;pl10 : tsatpwr - power level for 1H presat
;pl11 : power level for 1H 1 ms 90o pulse
;pl12 : tpwrml - power level for 1H waltz16 typically 40 us 1H pulse
;pl21 : power level for 13C decouping during acquisition
;pl24 : power level for Ca90b/CO90b
;pl25 : power level for CO180b/Ca180b
;pl26 : power level for 13C decoupling during nutation
;pl27 : power level for sel Cb decoupling
;pl3 :  power level for pwn
;pl31 : power level for 15N cpd No decoupling
```

;sp25 : power level for pwco180 (shaped pulse when carrier is on Ca)
;sp30 : power level for pwca180 (shaped pulse) when carrier is on CO
;p1 : pwh
;p11 : H pulse width at pl11 - use 1 ms and calibrate on water to get power
;p13 : pwh_soft - of duration exactly 1/4>JHN 2720 us
;p15 : first purge duration
;p16 : second purge duration
;p24 : pwc90
;p25 : pwc180
;p26 : pw90 for 13C decoupling during 1H nutation
;p27 : pwCbdec - pattern length us @ spw27
;p3 : pwn
;d1 : relaxation delay
;d11 : delay for disk i/o, 30ms
;d16 : gradient recovery delay, 200us
;d20 : taua, H to C, <=1.8ms
;d21 : taub, refocus JHC for 13C mag, 1.8 ms
;d22 : tauc, Ca to CO transfer, ~ 4.5 ms
;d24 : taue, N-CO J evolve, ~ 16.5 ms for unfolded proteins
;d27 : internal variable; do not adjust
;l15 : number of 1H frequencies to be used
;cpds1: 1H WALTZ decoupling defined according to program defined by cpdprg1 (waltz16)
;cpds2 : 13C decoupling according to program defined by cpdprg2 (waltz16)
;cpd3 : 15N decoupling according to program defined by cpdprg3 (waltz16)
;cpds7: Cb decoupling according to program defined by cpdprg7 (wurst2)
;pcpd2: 1/dmf - 90 degree pulse for cpd2
;pcpd3: 1/dmf2 - 90 degree pulse for cpd3
;cpdprg1 : File name for 1H waltz16
;cpdprg2 : File name for 13C decoupling during acq
;cpdprg5 : File name for 13C decoupling during 1H nutation
;cpdrgp7 : File name for 13Cb decoupling during 13Ca to 13CO transfer
;spnam25 : File name for D/sq(3), +118p
;spnam27 : File name for Cb decoupling during Ca to Co transfer
;spnam30 : File name for Ca D/sq(3), -118p
;zgoptns : Df1180, Df2180, DoneDarray, Dmess_flg, Dfsat, DN_flg, Dgd_sel, Dcal_HB1